Environmental and Molecular Mutagenesis 55:741–750 (2014)

Research Article

Induction of Macrophage Cell-Cycle Arrest and Apoptosis by Humic Acid

Hsin-Ling Yang,[1] Pei-Jane Huang,[2] Ssu-Ching Chen,[3] Hsin-Ju Cho,[1] K. J. Senthil Kumar,[4] Fung-Jou Lu,[5] Chih-Sheng Chen,[1] Chia-Ting Chang,[1] and You-Cheng Hseu[2,4]*

[1]*Institute of Nutrition, China Medical University, Taichung 40402, Taiwan*
[2]*Department of Health and Nutrition Biotechnology, Asia University, Taichung 41354 Taiwan*
[3]*Department of Life Sciences, National Central University, Chung-Li 32001, Taiwan*
[4]*Department of Cosmeceutics, College of Pharmacy, China Medical University, Taichung 40402, Taiwan*
[5]*Institute of Medicine, Chun Shan Medical University, Taichung 40201, Taiwan*

Humic acid (HA) in well water is associated with Blackfoot disease and various cancers. Previously, we reported that acute humic acid exposure (25–200 μg/mL for 24 hr) induces inflammation in RAW264.7 macrophages. In this study, we observed that prolonged (72 hr) HA exposure (25–200 μg/mL) induces cell-cycle arrest and apoptosis in cultured RAW264.7 cells. We also observed that exposing macrophages to HA arrests cells in the G_2/M phase of the cell cycle by reducing cyclin A/B_1, Cdc2, and Cdc25C levels. Treating macrophages with HA triggers a sequence of events characteristic of apoptotic cell death including loss of cell viability, morphological changes, internucleosomal DNA fragmentation, sub-G_1 accumulation. Molecular markers of apoptosis associated with mitochondrial dysfunction were similarly observed, including cytochrome *c* release, caspase-3 or caspase-9 activation, and Bcl-2/Bax dysregulation. In addition to the mitochondrial pathway, HA-induced apoptosis may also be mediated through the death receptor and ER stress pathways, as evidence by induction of Fas, caspase-8, caspase-4, and caspase-12 activity. HA also upregulates p53 expression and causes DNA damage as assessed by the comet assay. These findings yield new insight into the mechanisms by which HA exposure may trigger atherosclerosis through modulation of the macrophage-mediated immune system. Environ. Mol. Mutagen. 55:741–750, 2014.

Key words: blackfoot disease; humic acid; G2/M arrest; apoptosis; DNA damage

INTRODUCTION

Humic substances, which occur in the forms of humic acid, fulvic acid, and humin, exist in half of the world's well water. Humic acid (HA) is a high-molecular weight polymer that is primarily derived from biodegradation of dead organic matter. This dark-brown, carbon-rich material appears mostly in peat, soil, coal, upland streams, dystrophic lakes, and well water [Hartenstein, 1981]. The presence of these materials in drinking water is a precursor to undesirable trihalomethane formation during chlorination, with consequences that are detrimental to human health [Yang and Shang, 2004].

HA was identified as one of the potential causal factors contributing to an outbreak of Blackfoot disease (a peripheral vasculopathy) on the Southwest Coast of Taiwan in the 1970s [Hseu et al., 2002a]. Geochemical and epidemiologic studies revealed high HA concentrations (approximately 200 ppm) in artesian well water in the endemic areas [Lu, 1990], with daily average HA

Additional Supporting Information may be found in the online version of this article.

Grant sponsor: National Science Council, Taiwan; Grant number: NSC-101-2320-B-039-050-MY3.

*Correspondence to: You-Cheng Hseu, Department of Cosmeceutics, College of Pharmacy, China Medical University, 91 Huseh-Shih Road, Taichung 40402, Taiwan. E-mail: ychseu@mail.cmu.edu.tw
Hsin-Ling Yang and Pei-Jane Huang contributed equally to this work.

Received 6 February 2014; provisionally accepted 9 August 2014; and in final form 12 August 2014

DOI 10.1002/em.21897

Published online 2 September 2014 in Wiley Online Library (wileyonlinelibrary.com).

intake by residents estimated to be as high as 400 mg/day [Huang et al., 1995]. Contaminated well water consumed by local inhabitants is viewed as a possible cause of this outbreak [Lu, 1990]. Notably, the signs and symptoms of Blackfoot disease are similar to those of arteriosclerosis and Buerger's disease [Wang et al., 2007]. Increased mortality of cardiovascular and cerebrovascular diseases are also correlated with Blackfoot disease [Wang et al., 2007]. Following absorption in the gastrointestinal tract, HA can circulate in the blood [Hu et al., 2010]. Consuming excessive amounts of HA from well water could plausibly have adverse effects on human health, initiating Blackfoot disease pathogenesis and progression. However, the underlying pathophysiological mechanisms are poorly understood.

Macrophages are key immune effectors with vital roles in inflammation, host defense, and responses to a myriad of autologous and/or foreign invaders [Zhang et al., 2010]. However, uncontrolled and excessive activation of the macrophage inflammatory response may result in persistent swelling, pain, and eventual tissue injury [Karin et al., 2006]. Studies have demonstrated that acute exposure to toxins elicits an inflammatory response in macrophage cells, while extended/chronic exposure triggers macrophage apoptosis [Sakurai et al., 1998, 2006; Dutta et al., 2008; Zhao et al., 2009; Tabas, 2010]. These findings suggest that macrophages are useful for examining the impact of chemicals on mammalian immune systems.

Our previous study provided experimental support for the hypothesis that acute exposure to environmental HA triggers the inflammatory response and implicated HA as a factor in atherosclerosis and Blackfoot disease. HA exposure (24 hr) can produce atherosclerosis through the induction of proinflammatory mediators (TNF-α, IL-1β, NO, PGE2, iNOS, and COX-2) and the activation of NF-κB/AP-1 cascades via ROS generation and the AKT and MAPK signaling pathways in murine macrophages [Hseu et al., 2014]. The present study assessed the in vitro effects of extended (72 h) exposure of macrophage cells to HA and showed substantial inhibition of macrophage proliferation via cell-cycle arrest at the G_2/M transition phase. The extended HA exposure also induced apoptosis via the activation of the death-receptor, mitochondrial, and ER-stress signaling cascades. We believe this research will improve our understanding of HA involvement in the mortality of immune cells, which may be involved in cardiovascular and Blackfoot disease.

MATERIALS AND METHODS

Chemicals and Reagents

Dulbecco's modified Eagle's medium (DMEM), penicillin/streptomycin, and fetal bovine serum were obtained from Gibco/BRL Life Technologies (Grand Island, NY), while 3-[4,5-dimethyl-2-yl]-2,5-diphenyl tetrazolium bromide (MTT) was obtained from Sigma-Aldrich (St. Louis, MO). Antibodies against cytochrome *c*, Bcl-2, Bax, Fas, FasL, cyclin B1, Cdc2, p53, p-p53 (Ser20), and *β*-actin were obtained from Santa Cruz Biotechnology (Heidelberg, Germany), with antibodies against cyclin A, Cdc25C, caspase-9, caspase-3, PARP, and Bid obtained from Cell Signaling Technology (Danvers, MA). PARP rabbit polyclonal antibody was purchased from Roche (Mannheim, Germany). Antibodies against caspase-4 were purchased from Biomol (Montgomery, PA), antibodies against caspase-8 were purchased from NeoMarkers (Fremont, CA), antibodies against caspase-12 were purchased from Millipore (Billerica, MA), and 4′,6-diamidino-2-phenylindole dihydrochloride (DAPI) was purchased from Calbiochem (La Jolla, CA). All other chemicals were the highest commercially available grade and were obtained from either Merck & Co. (Darmstadt, Germany) or Sigma-Aldrich (St. Louis, MO).

Preparation of Synthetic HA

To eliminate impurities, HA was synthesized from monomeric protocatechuic acid according to a previously published procedure [Hseu et al., 2002c], with slight modifications. For oxidative polymerization, 1 g of protocatechuic acid in 100 mL of distilled water was oxidized with sodium periodate for 24 hr in a water bath at 50°C with gentle shaking. After centrifugation at 3000*g*, the supernatant was acidified to pH 1.0 using 0.1 N HCl. The acidified solution was again centrifuged, and its precipitate was treated with 0.1 N NaOH to solubilize HA, which was further purified by absorption chromatography with XAD-7 resin and fractionated by Sephadex G-25 chromatography, as detailed by Hseu et al. [2002c]. The HA solution was ultrafiltered through a Molecular/Por membrane (excluding particles <500 Da MW), and the resultant HA (500–10,000+ Da MW) was collected for further study. To prepare the stock solution, the synthetic HA was dissolved in phosphate buffered saline (PBS). The solution was stored at −20°C prior to use.

Cell Culture and Cell Viability Assay

The murine macrophage RAW264.7 cell line was obtained from the American Type Culture Collection (ATCC, Rockville, MD) and cultured in DMEM containing 4 mM glutamine and 10% heat-inactivated fetal bovine serum in a humidified 5% CO_2 atmosphere. Cell viability was assessed using the MTT colorimetric assay, as previously described [Hseu et al., 2014]. In brief, 4×10^4 cells/cm^2 were cultured in a 24-well plate for 72 hr with HA (25–200 μg/mL). As a negative control, an equal amount of PBS was substituted for HA in the culture medium. After incubation, the culture supernatant was removed and 400 μL of 0.5 mg/mL MTT in PBS was added to each well, followed by incubation at 37°C for 4 hr. MTT-generated farmazan crystals were dissolved in 400 μL of isopropanol, and the colorimetric absorbance was measured at 540 nm (A_{540}) with a microplate reader (Bio-Tek Instruments, Winooski, VT). Viability (%) was calculated as (A_{540} of treated cells/A_{540} of untreated cells) × 100.

Cell-Cycle Analysis

Cellular DNA content was determined by flow cytometry with propidium iodide (PI)-labeled cells. Briefly, macrophages (1.6×10^4 cells/cm^2) were cultured in 10 cm culture dishes with 10 mL medium. After HA treatment, the cells were harvested, washed with PBS and fixed in ice-cold 70% ethanol at −20°C overnight. Following incubation, the cells were re-suspended in PBS containing 1% Triton X-100, 0.5 mg/mL RNase, and 4 μg/mL PI at 37°C for 30 min. The DNA content of 1×10^4 cells/analysis was monitored using the FACSCalibur system (Becton Dickinson, San Jose, CA) equipped with a single argon-ion laser (488 nm), and analyzed using ModFit software (Verity Software House, Topsham, ME). Apoptotic nuclei were identified as subploid DNA peaks

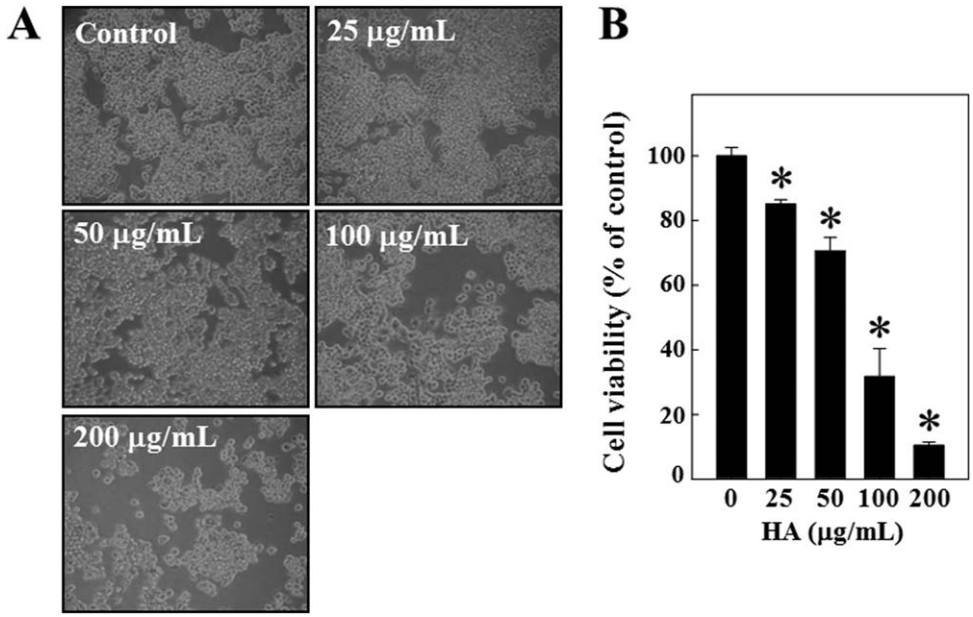

Fig. 1. HA inhibits RAW264.7 macrophage growth. Cells were treated with increasing HA (25–200 μg/mL) concentrations or vehicle alone (0.1% of PBS) for 72 hr. (**A**) Morphology under phase contrast microscope at 200× magnification. (**B**) Viability based on the MTT assay with values expressed as the mean ± SD ($n = 3$). *Significant difference compared to the control group ($P < 0.05$).

(as opposed to originating from cell debris) based on forward light scatter and PI fluorescence.

Apoptosis Determination

Apoptotic cell death was measured by terminal deoxynucleotidyl transferase-meditated dUTP-fluorescent nick end-labeling (TUNEL) with a fragmented DNA detection kit (Roche, Mannheim, Germany) following the supplier's instructions. Macrophages (4×10^4 cells/cm^2) were seeded on a 24-well culture plate with 1 mL medium and treated with HA (100 and 200 μg/mL) for 72 hr. Cells were washed twice with PBS, fixed in 2% paraformaldehyde for 30 min, permeabilized with 0.1% Triton X-100 for 30 min at room temperature, incubated with TUNEL reaction buffer at 37°C in a humidified chamber for 1 hr in the dark, then washed twice in PBS and incubated with DAPI (1 μg/mL) at 37°C for 5 min. Stained cells were visualized under a fluorescence microscope, and fluorescence intensity under each condition was quantified based on a squared section of fluorescence-stained cells using the analySIS LS 5.0 soft image solution (Olympus Imaging America, Corporate Parkway Centre Valley, PA). The fold increase of intensity was calculated by comparison to un-treated controls (which were arbitrarily assigned a value of onefold), and correlated directly with the number of apoptotic cells.

Western Blot

Macrophages (1.6×10^4 cells/cm^2) were incubated with various concentrations of HA (25–200 μg/mL) for 72 hr. After incubation, the cells were washed once in PBS, detached, suspended in lysis buffer (10 mM Tris–HCl [pH 8.0], 0.32 M sucrose, 1% Triton X-100, 5 mM EDTA, 2 mM DTT, and 1 mM phenylmethyl sulfonyl fluoride), then centrifuged at 15,000*g* for 30 min at 4°C. The protein content in the samples was quantified using a Bio-Rad assay reagent (Bio-Rad, Hercules, CA) with BSA as a standard. Proteins were mixed with buffer (62 mM Tris–HCl, 2% SDS, 10% glycerol, 5% β-mercaptoethanol), and samples were denatured at 97°C for 5 min. Equal amounts (50 μg) of denatured proteins were separated by SDS-PAGE (8–15%) and transferred to PVDF membranes overnight. Transferred membranes were blocked with 5% nonfat dried milk resuspended in PBS containing 1% Tween-20 for 1 hr at room temperature, followed by incubation with primary antibodies overnight, then incubated with either horseradish peroxidase-conjugated goat antirabbit or antimouse antibodies for 2 hr. Blots were detected with an ImageQuant LAS 4000 mini (Fujifilm) with SuperSignal West Pico chemiluminescence substrate (Thermo Scientific, IL).

Fluorescent Imaging of Mitochondrial Activity

Fluorescent mitochondrial imaging used MitoTracker® Green FM (Molecular Probe, Eugene, OR) according to the manufacturer's instructions. To label the mitochondria, cells were incubated with MitoTracker® probes, which passively diffuse across the plasma membrane and accumulate in active mitochondria. Cells (4×10^4 cells/cm^2) were seeded on a 24-well plate, treated with different HA concentrations (25–200 μg/mL) for 72 hr. After treatment, cells were fixed in 2% paraformaldehyde in PBS for 15 min and incubated with 1 μM MitoTracker for 30 min. A 1 μg/mL DAPI stain was applied for 5 min, and the stained cells were visualized by fluorescent microscopy at 400× magnification.

Single-Cell Gel Electrophoresis Assay (Comet Assay)

The comet assay is an uncomplicated and sensitive technique that detects DNA damage in individual eukaryotic cells [Zhao et al., 2009]. Macrophages (1×10^6 cells/10 cm dish) were incubated with increasing concentrations of HA (25–200 μg/mL) for 72 hr at 37°C. Cells were suspended in 1% low-melting point agarose in PBS (pH 7.4) and pipetted on to superfrost glass microscope slides precoated with a layer of 1% normal melting point agarose (warmed to 37°C before use). The agarose was allowed to set at 4°C for 10 min. Slides were immersed in lysis buffer containing 2.5 M NaCl, 100 mM EDTA, 10 mM Tris, and 1%

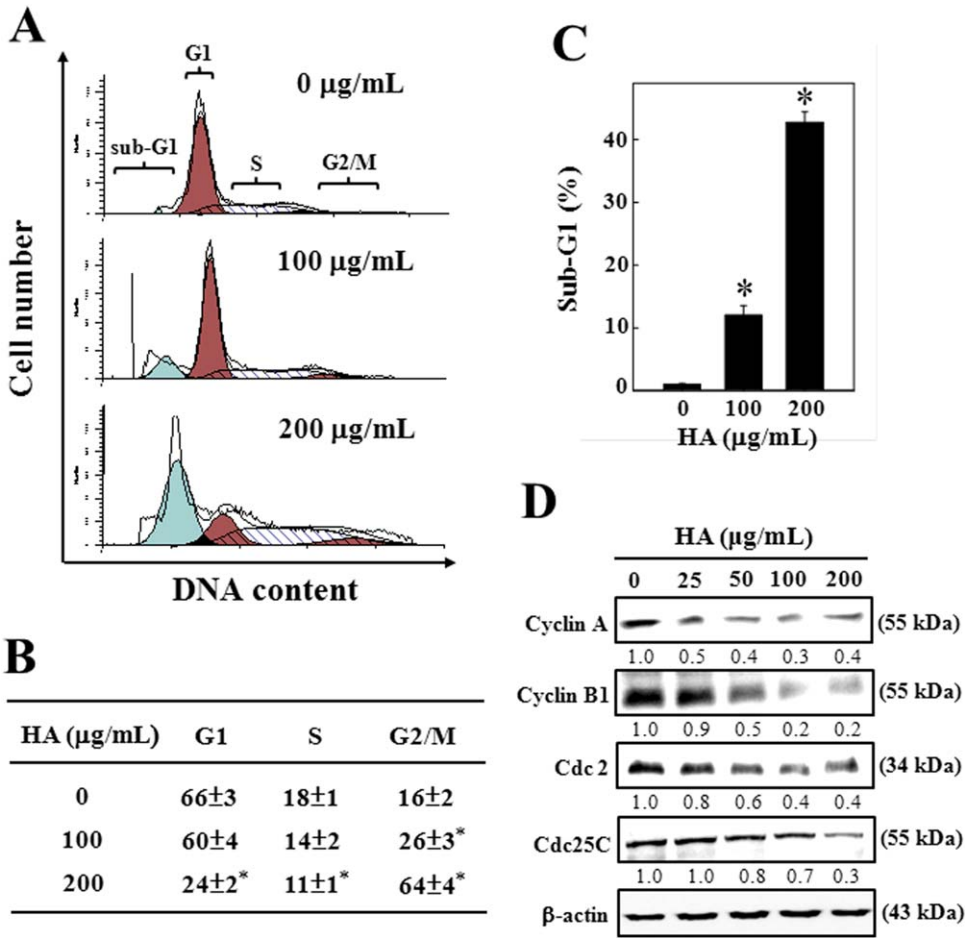

B

HA (μg/mL)	G1	S	G2/M
0	66±3	18±1	16±2
100	60±4	14±2	26±3*
200	24±2*	11±1*	64±4*

Fig. 2. HA induced sub-G_1 accumulation and G_2/M arrest in macrophages. (**A**) Cells were treated with HA (100 and 200 μg/mL) for 72 hr, stained with PI and analyzed by flow cytometry to determine their sub-G_1 and cell-cycle phases. (**B**) Apoptotic nuclei were identified as a subploid DNA peak and were distinguished from cell debris based on forward light scattering and PI fluorescence. (**C**) Cellular distribution (percentage) in cell-cycle phases (G_1, S, and G_2/M) after HA treatment. (**D**) Effects of HA (25–200 μg/mL) on cyclin A, cyclin B1, Cdc 2, and Cdc25C levels were monitored for 72 hr by Western blot, relative band intensity shown just below gel data. The results presented as the mean ± SD of three assays. *Significant difference in comparison to the control group ($P < 0.05$). [Color figure can be viewed in the online issue, which is available at wileyonlinelibrary.com.]

Triton X-100 at 4°C for 60 min, then placed in single rows inside a 30-cm wide horizontal electrophoresis tank containing 0.3 M NaOH and 1 mM EDTA (pH 13.4) at 4°C for 40 min to let the two DNA strands separate (alkaline unwinding). Electrophoresis was performed in an unwinding solution at 30 V (1 V/cm), 300 mA for 30 min, and slides were washed three times (5 min each) with 0.4 M Tris (pH 7.5) at 4°C and stained with propidium iodide (PI). The PI-stained nuclei were examined using a fluorescence microscope with a 510–550 nm excitation filter at 200× magnification.

DNA damage in the RAW264.7 cells, specified as DNA strand breaks comprising double and single-strand variants at alkali-labile sites, was analyzed under alkaline conditions (pH 13.4), comet scoring of cellular DNA on each slide was based on characterization of 100 randomly selected nucleoids. Apparent damage was not homogeneous; therefore, comet-like DNA formation was visually categorized into classes 0–4 representing increasing DNA damage in the "tail". The overall score for 100 comets ranged from 0 (100% of comets in class 0) to 400 (100% of comets in class 4), and the overall DNA damage in the cell population was expressed in arbitrary units [Zhao et al., 2009]. Observation and analysis of the results were always performed by the same experienced observer, who was blinded to the slide identity.

Statistics

Data are presented as the mean ± standard deviation (mean ± SD). All data were analyzed using ANOVA (analysis of variance), followed by Dunnett's test for pairwise comparison; significance was determined as $P < 0.05$ for all tests.

RESULTS

HA Inhibits Growth and Survival of RAW264.7 Cells

The effect of HA on RAW264.7 cell survival was assayed by exposing the cell to increased concentrations of HA (25, 50, 100, and 200 μg/mL) for 72 hr. The cell viability was observed with a bright field microscope. The reduction in cell number after exposed to HA clearly indicating the cytotoxicity effect of HA on RAW264.7 cells. MTT colorimetric assay further confirmed the HA-induced cell death (Fig. 1A). HA-induced significant

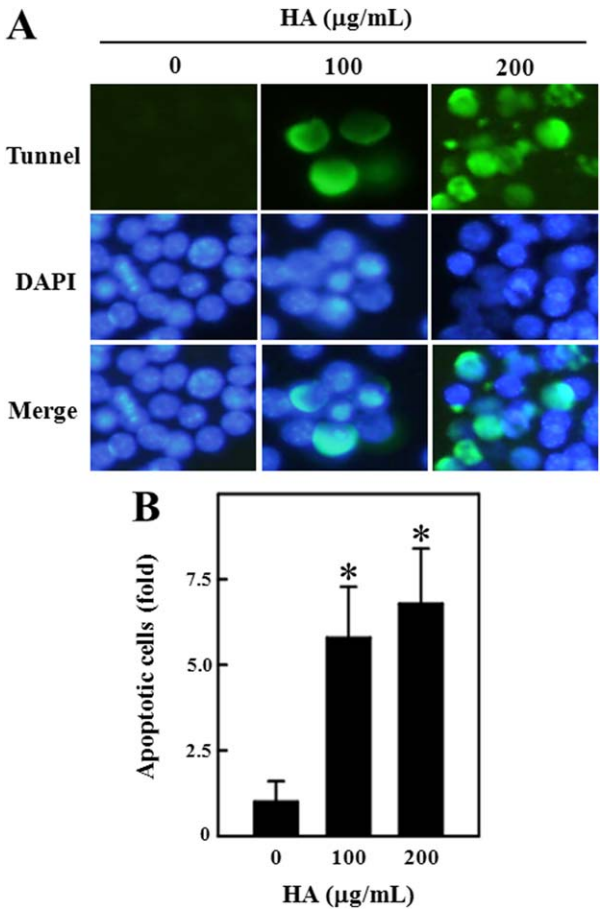

Fig. 3. HA induced apoptotic DNA fragmentation in macrophages. (**A**) TUNEL assay of the cells exposed to HA (100 μg/mL) for 72 hr. TUNEL-positive cells in the microscopic fields (magnification 400×). (**B**) Histogram plots fold-increase of apoptotic cells by fluorescence intensity, with results presented as the mean ± SD of three assays. *Significant difference compared to the control group ($P < 0.05$). [Color figure can be viewed in the online issue, which is available at wileyonlinelibrary.com.]

($P < 0.05$) dose-dependent drop in cell viability was found with the calculated IC_{50} of 96 μg/mL. More precisely, gradual decrease in cell viability was 84 ± 2, 71 ± 5, 29 ± 11, and $10 \pm 2\%$ with the dose of 25, 50, 100, and 200 μg/mL concentrations of HA, respectively (Fig. 1B). These results indicate that HA inhibits survival of RAW264.7 cells.

HA Induces Cell-Cycle Arrest at the G_2/M Transition Phase

The DNA content profile for the HA-treated RAW264.7 cells was obtained by flow cytometric analysis to measure the fluorescence yielded by PI binding to DNA. Figure 2A shows that HA exposure caused progressive and sustained accumulation of cells in the G_2/M transition phase. Additionally, HA treatment increased the proportion of cells that were in S and G_2/M phases, and decreased the proportion of cells in G_1 phase, in a concentration-dependent manner (Fig. 2B). The findings suggest that HA inhibits cell growth by inducing cell-cycle arrest at the G_2/M phase in macrophages. Furthermore, HA treatment resulted in a remarkable increase in the proportion of cells that were subploid (so-called sub-G_1 phase) from 2.6 to 41% (Fig. 2C). These subploid cells have lower DNA content relative to their diploid analogs indicative of apoptotic cells, which indicates a marked increase in apoptosis induced by HA treatment.

HA Down-Regulates Cyclin A, Cyclin B_1, Cdc2, and Cdc25C Expression in Macrophages

We investigated the effects of HA on various cyclins and CDKs that are involved in the regulation of cell-cycle in RAW264.7 cells. Western blotting demonstrated that HA exposure caused a dose-dependent reduction in cyclin A, cyclin B_1, mitotic cyclin-dependent kinase Cdc2, and mitotic phosphatase Cdc25C expressions (Fig. 2D). The molecular evidence implies that HA-induced reductions may contribute to inhibition of cell-cycle progression in RAW264.7 cells.

HA Induces Apoptotic DNA Fragmentation in Macrophages

HA-associated decrease in cell survival was further evaluated by assaying the apoptotic markers. For this assay, RAW264.7 cells were exposed to two different concentrations of HA (100 and 200 μg/mL) for 72 hr, and apoptotic DNA fragmentation of RAW264.7 cells was determined using the TUNEL assay. We found a dose-dependent increase in TUNEL-positive (green) cells, indicating that HA induces apoptosis in RAW264.7 cells (Fig. 3A). Specifically, apoptotic DNA fragmentation increased by 5.7 ± 1.6-fold and 7.1 ± 0.8-fold with the exposure of 100 and 200 μg/mL of HA, respectively (Fig. 3B).

HA Induces Cytochrome c Release, Caspase-9 or -3 Activation, and PARP Cleavage

Release of cytochrome *c* from mitochondria into the cytoplasm can be an early marker of apoptosis, which may in turn be caused by mitochondrial membrane damage due to exposure to environmental factors or chemical agents [Reed, 2000]. In this study, we measured the cytosolic and mitochondrial cytochrome *c* levels by western blot to determine the effect of 72 hr HA exposure on cytochrome *c* release. We found that HA treatment (25–200 μg/mL for 72 hr) showed a dose-dependent increase in cytosolic cytochrome *c* levels, whereas mitochondrial cytochrome *c* levels were decreased in RAW264.7 cells (Fig. 4A). Given that cytochrome *c* is involved in activating caspases that trigger the apoptosis [Reed, 2000], we investigated the roles of caspase-9 and caspase-3 in response to HA exposure. Western blot analyses show that HA treatment induced proteolytic cleavage of procaspase-9 and -3 into

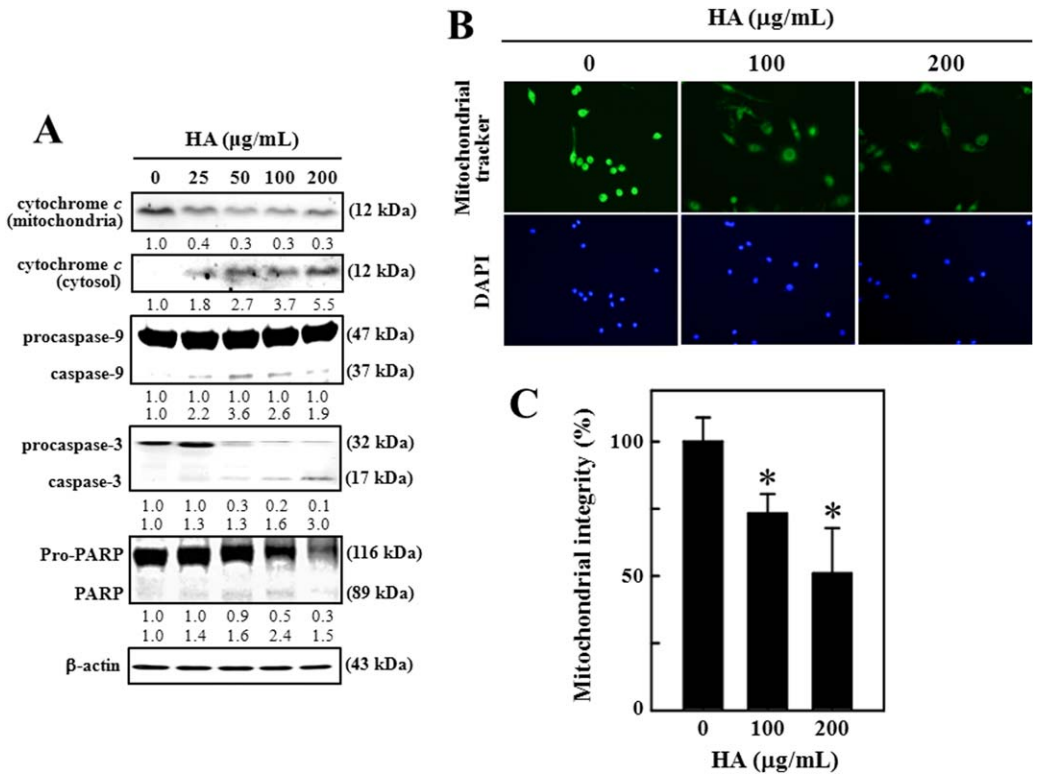

Fig. 4. HA induces apoptosis via a mitochondria-dependent pathway. (**A**) Western blot analysis of apoptosis-related proteins (mitochondrial and cytosolic cytochrome *c*, caspase-9 or −3, and PARP) in macrophages exposed to HA (25–200 μg/mL) for 72 hr, with relative band intensity shown below the gel data. (**B**) Effect on macrophage mitochondrial activity, rated by tracking Mito-Tracker FM uptake (green CMXRos) into mitochondria. After 72 hr HA (25–200 μg/mL) treatment, RAW264.7 cells were incubated for 30 min with 1 μM Mito-Tracker at 37°C, DAPI (1 μg/mL) stained for 5 min and examined by fluorescent microscopy (magnification 400×); see "Materials and Methods". (**C**) The percentage of mitochondrial activity was analyzed by densitometry, with the results presented as the mean ± SD of three assays. *Significant difference in comparison to the control group ($P < 0.05$). [Color figure can be viewed in the online issue, which is available at wileyonlinelibrary.com.]

their active forms. Furthermore, addition of HA resulted in proteolytic cleavage of the 116 kDa PARP protein to 89 kDa fragment. Cleavage of PARP by activated caspase-3 in this study appears to be a biochemical index of apoptosis, which suggesting that HA-induced apoptosis is mediated by a mitochondria-dependent pathway.

Mitochondrial Membrane Permeability in Response to HA Treatment

To confirm whether HA-induced apoptosis is associated with a loss of mitochondrial membrane potential, we examined HA-induced mitochondrial injury in RAW264.7 cells using the Mito-Tracker assay kit. Mito-Tracker is a green fluorescent dye that stains mitochondria in live cells in a mitochondrial membrane potential-dependent manner. The images presented in Figure 4B shows that control cell possess bright green fluorescence, while HA treatment significantly reduced the intensity of the green fluorescence. The decreased fluorescence intensity was 74 ± 6 and 51 ± 18% with exposure of 100 and 200 μg/mL of HA, respectively. These data indicate that mitochondrial integrity is severely impaired by HA in RAW264.7 cells.

HA Mediates Bcl-2 and Bax Protein Dysregulation

Bcl-2 is a potent inhibitor of apoptosis, whereas Bax is a proapoptotic protein that acts by forming a heterodimer with Bcl-2, thereby inhibiting Bcl-2 activity [Singh, 2007]. Bcl-2 and Bax protein levels were thus studied in cultured RAW264.7 cells for their involvement in HA-mediated apoptosis. The estimated antiapoptotic Bcl-2 protein was dramatically downregulated, while proapoptotic Bax protein was upregulated by HA exposure (Fig. 5A). The Bax/Bcl-2 ratio was remarkably high with high concentrations of HA (100 and 200 μg/mL) (Fig. 5B). The results clearly indicate that altered Bcl-2 and Bax proteins by HA could enhance apoptosis in RAW264.7 cells.

HA Activates Fas-Mediated Apoptosis through the Activation of Caspase-8 and Cleavage of Bid

To ascertain whether HA (25–200 μg/mL for 72 hr) promotes apoptosis in RAW264.7 macrophages via a receptor-mediated pathway, Fas protein levels were assessed by western blot. HA markedly increased the Fas protein expression (Fig. 6A), and this increase was

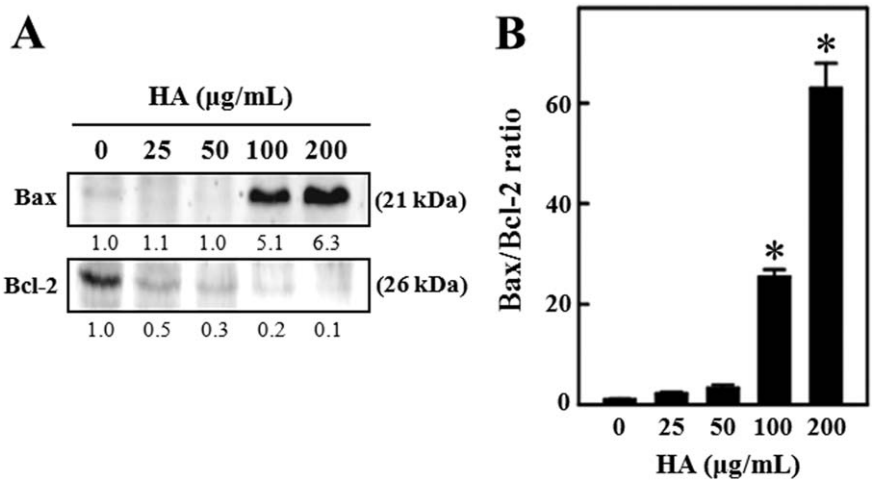

Fig. 5. Effect of HA on Bax/Blc-2 ratio in macrophages. (**A**) Western blot of anti-apoptotic Bcl-2 and proapoptotic Bax levels after exposing macrophages to HA. (**B**) Relative changes in Bcl-2 and Bax bands were analyzed by densitometry, with the results presented as the mean ± SD of three assays. *Significant difference in comparison to the control group ($P < 0.05$).

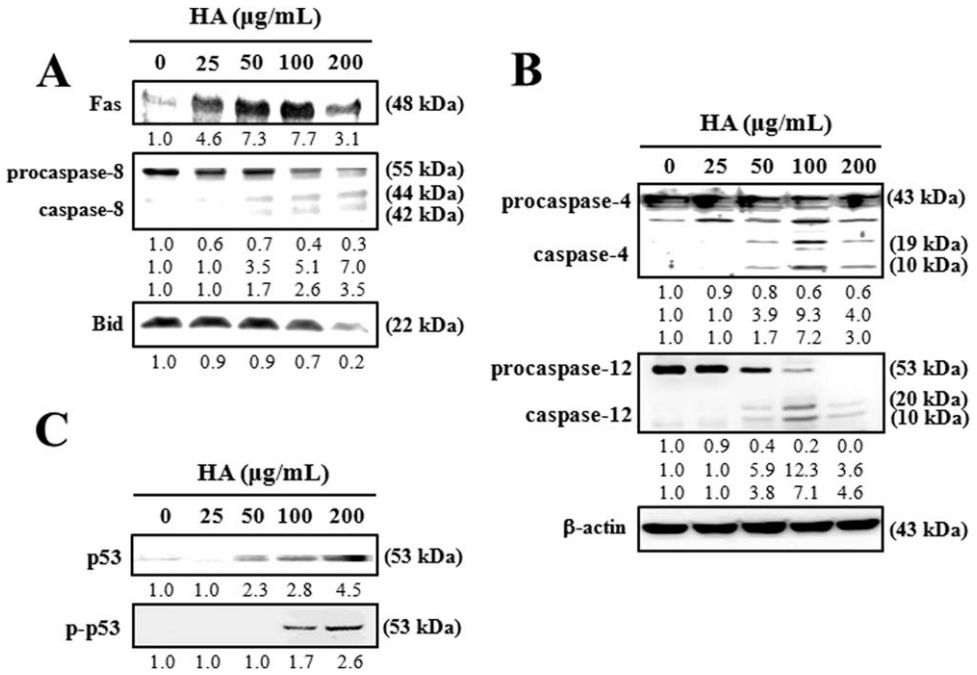

Fig. 6. HA induces apoptosis in macrophages via death receptor-, ER stress- and p53-dependent pathways. Macrophages were exposed to HA (25–200 μg/mL) for 72 hr. Protein expression levels of (**A**) Fas, caspase-8, and Bid (death receptor pathway); (**B**) caspase-4 and -12 (ER stress pathway); (**C**) p53 and p-p53 were monitored using specific antibodies, with relative band intensity shown just below the gel data.

associated with increased caspase-8 and decreased procaspase-8, consistent with HA-induced proteolytic activation of caspase-8 (Fig. 6A). Moreover, the expression levels of the proapoptotic Bid protein, which produces truncated Bid fragment (tBid) upon cleavage by caspase-8, were measured to determine whether HA treatment induces Bid cleavage in RAW264.7 cells (Fig. 6A). The data provide additional evidence that HA-induced apoptosis is also mediated by the death receptor pathway.

ER Stress is Involved in HA-Induced RAW264.7 Cell Apoptosis

To elucidate the role of endoplasmic reticulum (ER) stress in HA-induced apoptosis, we measured the

A

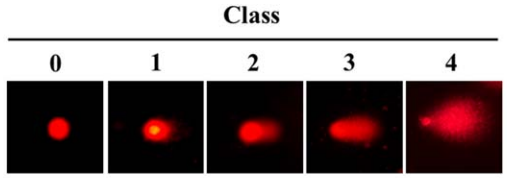

B

HA (μg/mL)	Toxicity scale					Total damage
	0	1	2	3	4	
0	97±1	3±1	0±0	0±0	0±0	3±1
25	38±4	20±3	22±2	19±1	1±2	125±11
50	32±4	8±5	23±6	22±3	15±3	180±6*
100	0±0	15±5	21±3	36±5	28±5	276±15*
200	0±0	0±0	0±0	24±3	76±3	376±3*

Fig. 7. HA damages macrophage DNA. RAW264.7 cells were treated with HA (25–200 μg/mL) for 72 hr. (**A**) DNA stained with PI under fluorescent photomicroscope. (**B**) Comet-like DNA formations were categorized as classes 0–4 to designate increasing DNA damage in the "tail" form, each assigned a value according to class. The overall score for 100 comets ranged from 0 (100% of class 0) to 400 (100% of class 4). The results are expressed as the mean ± SD of three assays. *Significant difference as compared to the control group ($P < 0.05$). [Color figure can be viewed in the online issue, which is available at wileyonlinelibrary.com.]

activation levels of caspase-4 and caspase-12 [Binet et al., 2010]. Exposure of RAW264.7 cells to the different concentrations of HA (25–200 μg/mL) for 72 hr had increased the proteolytic cleavage of procaspase-4 and procaspase-12 (Fig. 6B), indicating that HA-induced ER-stress could trigger apoptosis.

Induction of p53 and p-p53 Protein Expression by HA

The tumor suppressor gene p53 acts as a transcription factor to regulate DNA repair, cell death, and cell proliferation. p53 may function as a sensor for DNA damage that could arrest the cell-cycle for DNA repair, or upregulate proapoptotic factors, increasing susceptibility to apoptosis [Ryan et al., 2001]. Moreover, p53 tumor suppressor induction has been implicated in cell growth and apoptosis. The effects of HA (25–200 μg/mL) on p53 and p-p53 protein levels were therefore investigated in RAW246.7 cells over 72 hr. HA treatment increased both p53 and p-p53 protein levels in a dose-dependent manner (Fig. 6C), suggesting that HA-mediated p53 activation is associated with cell-cycle arrest and apoptosis in RAW264.7 cells.

HA Induces DNA Damage

The HA-induced cellular DNA damage was evaluated using comet assay, which reports on levels of single-strand DNA breaks. For this assay, the toxicity scale was generated by considering five classes of comet-like DNA formation representing increasing DNA damage (Fig. 7A). Our results show a dose-dependent increase in comet length with HA treatment (Fig. 7B), which clearly indicates that HA treatment enhances DNA damage in RAW264.7 cells.

DISCUSSION

Humic substances, found in half of the world's well water [Seo et al., 2013], are classified as humic acids (HA), fulvic acids, and humin, based on their pH and water solubility [Man et al., 2013]. HA has been suggested as an etiological factor in the development of vascular diseases in Blackfoot disease-endemic regions of Taiwan. Our previous study used an in vitro model of macrophage inflammation (25–200 μg/mL of HA for 24 hr), and found that activated macrophages produce proinflammatory molecules by activating transcriptional factors such as NF-κB and AP-1 [Hseu et al., 2014]. The current study explored the impact of an extended 72 hr HA exposure, and the resulting G_2/M arrest and mitochondrial-, death receptor-, and ER stress-mediated macrophage apoptosis (Supporting Information Fig. 1S).

Macrophage apoptosis occurs throughout all stages of atherosclerosis development. In late stages, a number of factors contribute to defective phagocytic clearance of apoptotic macrophages, producing secondary necrosis in these cells and a proinflammatory response [Tabas, 2010]. The present study suggests that not only does HA possess potential immunotoxicity, but also that extended HA exposure induces G_2/M cell-cycle arrest and apoptosis in macrophages. Given the presence of HA in drinking well water, additional mechanistic and epidemiological investigations should be undertaken explore the role of HA in atherosclerosis susceptibility further [Lu, 1990; Hseu and Yang, 2002; Hseu et al., 2000, 2002a, b, 2008]. We suggest that HA-induced macrophage apoptosis is an underlying mechanism involved in atherosclerosis in Blackfoot disease-endemic regions of Taiwan.

Eukaryotic cell-cycle progression involves sequential activation of CDKs in concert with cyclins [Bloom and Cross, 2007]. Among CDKs that regulate cell-cycle progression, CDK2 and Cdc2 kinases are primarily activated together with cyclins A and B_1 at G_2/M phase [Bloom and Cross, 2007]. Phosphorylation of Cdc2 suppresses Cdc2/cyclin A and B_1 kinase complex activity; its dephosphorylation is catalyzed by Cdc25C phosphatase, a reaction viewed as a rate-limiting step for entry into mitosis [Lim and Kaldis, 2013]. Our study used flow cytometry analysis to clearly demonstrate that HA treatment has a profound effect on cell-cycle progression, as evidenced by the accumulation of cells during the G_2/M phase transition. We assume that this cell-cycle blockade is associated with inhibition of cell-cycle regulatory proteins and their kinase activity. Indeed, expression levels of cyclin A/B, Cdc2, and Cdc25C were all downregulated in HA-treated in macrophages, consistent with G_2/M arrest.

The present study suggests that HA induces macrophage apoptosis via mitochondrial, death receptor, and ER stress pathways. Mitochondrial dysfunction, including the loss of mitochondrial membrane potential ($\Delta\Psi_m$) and

the release of cytochrome *c* from mitochondria into the cytosol, are associated with apoptosis [Ly et al., 2003]. Cytosolic cytochrome *c* activates procaspase-9, which in turn activates caspase-3 (among other targets), triggering apoptosis [Jiang and Wang, 2004]. In this study, exposing macrophages to HA induced mitochondrial membrane damage and released cytochrome *c* into the cytoplasm; it also activated procaspase-9 and -3. One target of caspse-3 is PARP. Prolonged activation of PARP may induce DNA damage by upregulating cellular NAD and ATP levels [Soldani and Scovassi, 2002]. Our results indicate that HA activates PARP DNA repair enzymes in macrophages.

The Bcl-2 gene family in mammalian cells generates anti-apoptotic proteins such as Bcl-2 and Bcl-xL, which are evidently involved in resistance to conventional cancer therapy. By contrast, proapoptotic proteins from the same gene family, including Bax, can induce apoptotic cell death. Apoptosis largely depends on a balance between anti- and proapoptotic proteins [Kuwana and Newmeyer, 2003]. The present study suggests that HA treatment disrupts the Bcl-2/Bax ratio leading to macrophage apoptosis.

In addition to the Bcl-2/Bax apoptosis pathway, membrane death receptors, including Fas, are activated by their respective ligands to engage adaptor molecules and caspases including proximal caspase-8. Activated caspase-8 further stimulates caspase-3 via mitochondria-dependent cascades [Schmitz et al., 2000]. In the mitochondrial apoptosis pathway, caspase-8 proteolytically activates proapoptotic protein Bid, which targets mitochondrial membrane permeabilization and constitutes a primary link between extrinsic and intrinsic apoptotic pathways [Schug et al., 2011]. We observed that HA treatment stimulates Fas activity and activates both caspase-8 and Bid within macrophages. Finally, ER stress-induced apoptosis has its own signaling pathway that is independent of mitochondria and death receptors and is thought to be mediated by caspase-12 [Li et al., 2006]. Caspase-12 putatively activates caspase-9 independent of Apaf-1, followed by activation of caspase-3. Human caspase-4 is involved in the ER stress-induced cell death pathway as an alternative to caspase-12 [Szegezdi et al., 2006]. Our data show that HA-induced macrophage apoptosis is also mediated by the ER stress pathway as evidenced by caspase-4 and -12 activation.

ROS generation is one of several proposed mechanisms of action for HA-induced toxicity. We previously demonstrated HA exposure upregulates ROS and/or RNS production and apoptosis in various human cells to aggravate inflammation and atherosclerosis [Hseu et al., 2002a, b, 2008]. HA-induced ROS generation may trigger mitochondrial pathways, such as activation of p53 (as a sensor of DNA damage) that could in turn arrest the cell cycle for DNA repair or upregulate proapoptotic factors and heighten susceptibility [Ryan et al., 2001]. Our findings suggest that p53 mediates HA-induced cell-cycle arrest and/or macrophage apoptosis. The underlying mechanism of HA induction of p53 upregulation remains unclear; ROS generation and DNA damage warrant further study.

Substantial effort has been devoted to elucidating the molecular basis of Blackfoot disease associated with HA-related atherogenic potential, but no mechanism has been unequivocally established to date. Our results provide mechanistic evidence demonstrating that HA induces G_2/M cell-cycle arrest and apoptosis in macrophages. This HA-induced macrophage apoptosis is associated with mitochondrial, death receptor, and ER stress pathways. Considering the ubiquitous environmental presence of HA, this study provides new insight into the physiological and immunological effects caused by long-term exposure to HA.

ACKNOWLEDGMENTS

This work was funded by grants CMU 98-P-05-M, CMU 100-ASIA-13, and CMU 100-ASIA-14 from the Asia University and China Medical University of Taiwan.

AUTHOR CONTRIBUTIONS

You-Cheng Hseu, Fung-Jou Lu, and Ssu-Ching Chen designed the experiments, and Hsin-Ju Cho, Chih-Sheng Chen, and Chia-Ting Chang conducted the experiments. K.J. Senthil Kumar and You-Cheng Hseu prepared the manuscript, and Hsin-Ling Yang and Pei-Jane Huang organized the data and prepared the tables and figures.

REFERENCES

Binet F, Chiasson S, Girard D. 2010. Evidence that endoplasmic reticulum (ER) stress and caspase-4 activation occur in human neutrophils. Biochem Biophys Res Commun 391:18–23.

Bloom J, Cross FR. 2007. Multiple levels of cyclin specificity in cell-cycle control. Nat Rev Mol Cell Biol 8:149–160.

Dutta R, Mondal AM, Arora V, Nag TC, Das N. 2008. Immunomodulatory effect of DDT (*bis*[4-chlorophenyl]-1,1,1-trichlorethane) on complement system and macrophages. Toxicology 252:78–85.

Hartenstein R. 1981. Sludge decomposition and stabilization. Science 212:743–749.

Hseu YC, Yang HL. 2002c. The effects of humic acid–arsenate complexes on human red blood cells. Environ Res 89:131–137.

Hseu YC, Lu FJ, Engelking LR, Chen CL, Chen YH, Yang HL. 2000. Humic acid-induced echinocyte transformation in human erythrocytes: Characterization of morphological changes and determination of the mechanism underlying damage. J Toxicol Environ Health A 60:215–230.

Hseu YC, Huang HW, Wang SY, Chen HY, Lu FJ, Gau RJ, Yang HL. 2002a. Humic acid induces apoptosis in human endothelial cells. Toxicol Appl Pharmacol 182:34–43.

Hseu YC, Wang SY, Chen HY, Lu FJ, Gau RJ, Chang WC, Liu TZ, Yang HL. 2002b. Humic acid induces the generation of nitric oxide in human umbilical vein endothelial cells: Stimulation of nitric oxide synthase during cell injury. Free Radic Biol Med 32: 619–629.

Hseu YC, Chen SC, Chen YL, Chen JY, Lee ML, Lu FJ, Wu FY, Lai JS, Yang HL. 2008. Humic acid induced genotoxicity in human peripheral blood lymphocytes using comet and sister chromatid exchange assay. J Hazard Mater 153:784–791.

Hseu YC, Kumar KJS, Chen CS, Cho HJ, Lin SW, Shen PC, Lin CW, Lu FJ, Yang HL. 2014. Humic acid in drinking well water induces inflammation through reactive oxygen species generation and activation of nuclear factor-κB/activator protein-1 signaling pathways: A possible role in atherosclerosis. Toxicol Appl Pharmacol 274:249–262.

Huang, TS, Lu FJ, Tsai CW. 1995. Tissue distribution of absorbed humic acids. Environ Geochem Health 17:1–4.

Hu CW, Yen CC, Huang YL, Pan CH, Lu FJ, Chao MR. 2010. Oxidatively damaged DNA induced by humic acid and arsenic in maternal and neonatal mice. Chemosphere 79:93–99.

Jiang X, Wang X. 2004. Cytochrome *C*-mediated apoptosis. Annu Rev Biochem 73:87–106.

Kuwana T, Newmeyer DD. 2003. Bcl-2-family proteins and the role of mitochondria in apoptosis. Curr Opin Cell Biol 15:691–699.

Li J, Lee B, Lee AS. 2006. Endoplasmic reticulum stress-induced apoptosis: multiple pathways and activation of p53-up-regulated modulator of apoptosis (PUMA) and NOXA by p53. J Biol Chem 281:7260–7270.

Lim S, Kaldis P. 2013. Cdks, cyclins and CKIs: roles beyond cell cycle regulation. Development 140:3079–3093.

Lu FJ. 1990. Blackfoot disease: Arsenic or humic acid? Lancet 336: 115–116.

Ly JD, Grubb DR, Lawen A. 2003. The mitochondrial membrane potential (deltapsi(m)) in apoptosis; an update. Apoptosis 8:115–128.

Man D, Pisarek I, Braczkowski M, Pytel B, Olchawa R. 2013. The impact of humic and fulvic acids on the dynamic properties of liposome membranes: The ESR method. J Liposome Res. doi: 10.3109/08982104.2013.839998.

Reed JC. 2000. Mechanisms of apoptosis. Am J Pathol 157:1415–1430.

Ryan KM, Phillips AC, Vousden KH. 2001. Regulation and function of the p53 tumor suppressor protein. Curr Opin Cell Biol 13:332–337.

Sakurai T, Kaise T, Matsubara C. 1998. Inorganic and methylated arsenic compounds induce cell death in murine macrophages via different mechanisms. Chem Res Toxicol 11:273–283.

Sakurai T, Ohta T, Tomita N, Kojima C, Hariya Y, Mizukami A, Fujiwara K. 2006. Evaluation of immunotoxic and immunodisruptive effects of inorganic arsenite on human monocytes/macrophages. Int Immunopharmacol 6:304–315.

Schmitz I, Kirchhoff S, Krammer PH. 2000. Regulation of death receptor-mediated apoptosis pathways. Int J Biochem Cell Biol 32:1123–1136.

Schug ZT, Gonzalvez F, Houtkooper RH, Vaz FM, Gottlieb E. 2011. BID is cleaved by caspase-8 within a native complex on the mitochondrial membrane. Cell Death Differ 18:538–548.

Seo SB, Jin HX, Lee HY, Ge J, King JL, Lyoo SH, Shin DH, Lee SD. 2013. Improvement of short tandem repeat analysis of samples highly contaminated by humic acid. J Forens Leg Med 20:922–928.

Singh N. 2007. Apoptosis in health and disease and modulation of apoptosis for therapy: An overview. Indian J Clin Biochem 22:6–16.

Soldani C, Scovassi AI. 2002. Poly(ADP-ribose) polymerase-1 cleavage during apoptosis: An update. Apoptosis 7:321–328.

Szegezdi E, Logue SE, Gorman AM, Samali A. 2006. Mediators of endoplasmic reticulum stress-induced apoptosis. EMBO Rep 7:880–885.

Tabas I. 2010. Macrophage death and defective inflammation resolution in atherosclerosis. Nat Rev Immunol 10:36–46.

Wang CH, Hsiao CK, Chen CL, Hsu LI, Chiou HY, Chen SY, Hsueh YM, Wu MM, Chen CJ. 2007. A review of the epidemiologic literature on the role of environmental arsenic exposure and cardiovascular diseases. Toxicol Appl Pharmacol 222:315–326.

Yang X, Shang C. 2004. Chlorination byproduct formation in the presence of humic acid, model nitrogenous organic compounds, ammonia, and bromide. Environ Sci Technol 38:4995–5001.

Zhang Q, Wang C, Sun L, Li L, Zhao M. 2010. Cytotoxicity of lambda-cyhalothrin on the macrophage cell line RAW 264.7. J Environ Sci (China) 22:428–432.

Zhao M, Zhang Y, Wang C, Fu Z, Liu W, Gan J. 2009. Induction of macrophage apoptosis by an organochlorine insecticide acetofenate. Chem Res Toxicol 22:504–510.